Study of the Inhibitory Effect of Water-Soluble Fullerenes on Plant Growth at the Cellular Level

Qiaoling Liu,[†,§] Yuanyuan Zhao,[‡,§] Yinglang Wan,[‡] Junpeng Zheng,[†] Xuejie Zhang,[†] Chunru Wang,[†] Xiaohong Fang,[†,*] and Jinxing Lin*[,‡]

[†]Beijing National Laboratory for Molecular Sciences, Key Laboratory of Molecular Nanostructures and Nanotechnology, Institute of Chemistry, Chinese Academy of Sciences, Beijing 100190, People's Republic of China, and [‡]Institute of Botany, Chinese Academy of Sciences, Beijing 100093, People's Republic of China. [§]These authors contributed equally to this work.

ABSTRACT The effect of water-soluble fullerene $C_{70}(C(COOH)_2)_{4-8}$ on plant growth was investigated, using the transgenic seedling lines expressing fluorescent makers. The retarded roots with shortened length and loss of root gravitropism were observed for seedlings grown in the fullerene-containing medium. Fluorescence imaging revealed the abnormalities of root tips in hormone distribution, cell division, microtubule organization, and mitochondrial activity. The study of the inhibitory effects at the cellular level provides new information on the phytotoxicity mechanism of fullerene.

KEYWORDS: fullerenes · fluorescence imaging · phytotoxicity · green fluorescence protein · transgenic plants

The rapid development of nanomaterials has led to a growing need for investigating their potential impacts on human health and environment.[1] Up to now, most nanotoxicity studies have been focused on mammalian cells, bacteria, and animals.[2−4] Studies of the effect of nanomaterials on plants, an important and fundamental ecological component, are rare.[5−8] Limited reports on the phytotoxicity of nanomaterials proposed both negative and positive effects on plant development. For example, Al and ZnO nanoparticles were found to retard the growth of plant roots,[5,6] while carbon nanotubes were reported to promote the seed germination and growth.[7,8] The phytotoxicity mechanisms of those nanoparticles are still largely unknown. Apart from the passive exposure of plants to nanomaterials, there is an increasing interest in exploring the application of nanoparticles as delivery systems and imaging agents for plant cells and plants.[9−14] Therefore, more studies with different nanomaterials and different plant species are required, especially the studies at the cellular level, for the understanding of the phytotoxicity mechanisms, which has been rarely investigated in previous reports.

Fullerene is one of the most popular nanomaterials and has wide applications in different fields such as optics, electronics, cosmetics, and biomedicine,[15] yet its phytotoxicity has not been reported. In this work, we intended to investigate the effect of the water-soluble fullerene malonic acid derivative (FMAD), $C_{70}(C(COOH)_2)_{4-8}$, on the growth of a model plant, *Arabidopsis thaliana*. A new strategy of using transgenic lines which were stably transformed with green fluorescent protein (GFP) tagged markers was applied. This technique not only enabled the observation of the morphological changes of the plant seedlings in the presence of fullerene, but also realized the real-time imaging of certain cellular events by fluorescence microscopy for phytotoxicity mechanism study.

RESULTS AND DISCUSSION

FMAD Repressed the Growth of *Arabidopsis*. Water-soluble $C_{70}(C(COOH)_2)_{4-8}$ (FMAD) was first prepared by the established procedure, which generates 4 to 8 carboxyl groups on the fullerene cage.[16] FMAD tended to form monodisperse aggregates with sizes ranging from 100 to 200 nm, as characterized by atomic force microscopy and dynamic light scattering (Figure S1, Supporting Information).

The sterile *Arabidopsis thaliana* seeds were placed on agar with half-strength of standard Murashige and Skoog medium (half-strength MS medium) supplemented by different concentrations of FMAD (from 0.005 to 0.2 mg/mL). The half-strength MS medium without FMAD was used for control experiments. As shown in Figure 1A, after 5-day growth under FMAD treatment, the seedling roots were retarded with

*Address correspondence to xfang@iccas.ac.cn, linjx@ibcas.ac.cn.

Received for review June 24, 2010 and accepted September 27, 2010.

Published online October 6, 2010. 10.1021/nn101430g

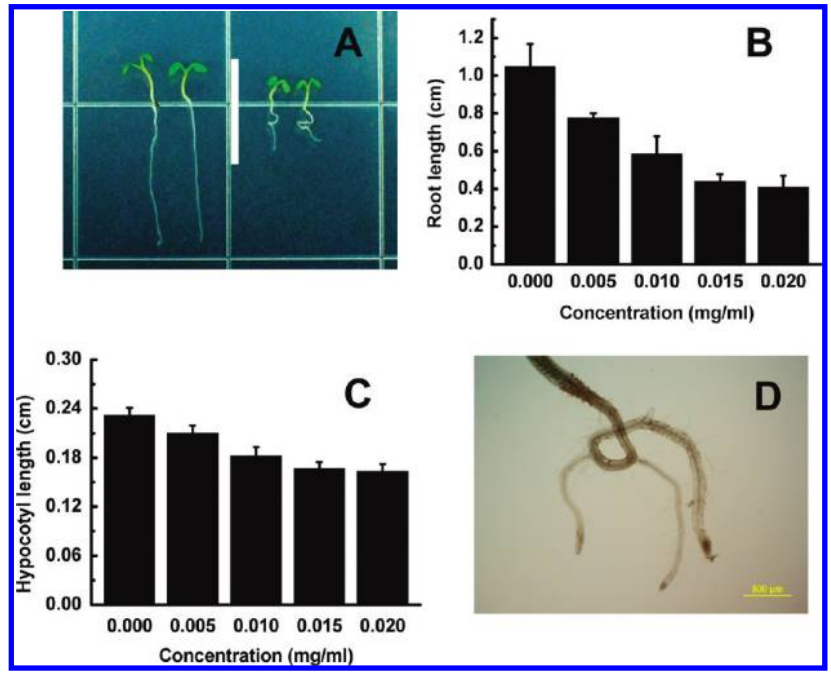

Figure 1. Effect of FMAD on seedling growth. 5-day old seedlings grown in the normal medium (A, left of the white bar) and the medium containing 0.01 mg/mL FMAD (A, right of the white bar) were imaged. The effect of FMAD on seedling root and hypocotyl elongation is concentration dependent (B, C). Lateral roots were formed and illustrated in the microscopy image (D). The scale bar is 500 μm for panel D.

obviously shorter length than the control and the repression became more serious with increasing concentration of FMAD (Figure 1B,C). In addition, new lateral roots were formed when the FMAD concentration was higher than 0.02 mg/mL (Figure 1D). Hypocotyls were shorter in length under the treatment of FMAD but the change was not as significant as that of roots. In our study, the seed germination rate was not affected by FMAD (data not shown).

It is expected that the selectively permeable seed coat provides the protection of seed from FMAD during the germination.[17] As radicle (the embryonic root) could contact with FMAD directly after penetrating the seed coat, root was the major organ to confront FMAD during the seedling growth. Therefore, the toxic symptoms were more significant in root than in other parts of seedlings. This was further confirmed by the evidence that the root growth of the seedlings, which had been cultured in the normal conditions for 5 days, was also retarded in root elongation after they were transferred to the medium containing FMAD (Figure S2, Supporting Information). Besides the shortened length, we observed the swollen root tips and the loss of gravitropism, the typical characteristics of root, for the seedlings treated by FMAD (Figure S3, Supporting Information).

As root is the most sensitive organ in response to FMAD in plant seedlings, we further investigated the growth of the seedling roots at the cellular level by fluorescence imaging to understand the inhibitory mechanisms. After the 5-day old seedlings were removed from the agar plate, the seedling roots were directly imaged under the confocal fluorescence microscope. Different locations in each root tip from its tip end to above were checked respectively to examine the transport of plant growth hormone at the root cap, the cell division in the root meristematic zone, and the microtubule array in epidermal cells in the root elongation zone.

FMAD Disrupted the Auxin Distribution in the Root Cap. To investigate the transport of plant growth hormone at the root cap, *Arabidopsis* seedlings transformed by *proDR5::GFP*, a fluorescent reporter expressing GFP in the presence of plant hormone auxin (indole-3-acetic

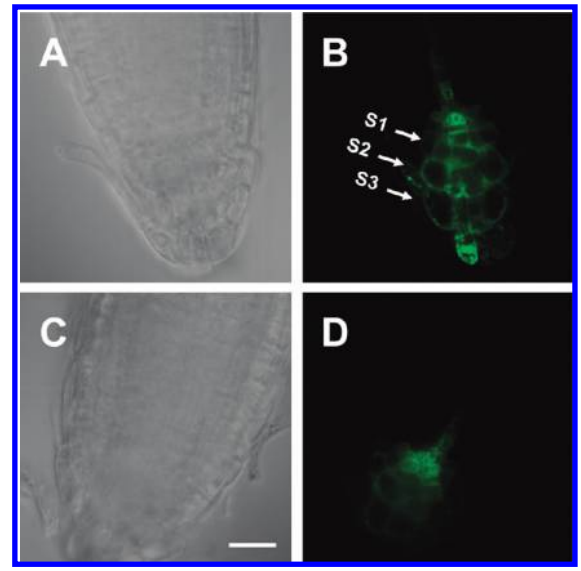

Figure 2. Optical and fluorescence images of *proDR5::GFP* transformed *Arabidopsis* grown in the medium without (A, B) and with (C, D) 0.01 mg/mL FMAD. Arrows indicate S1 to S3 layers in the columella root cap. The scale bar is 20 μm.

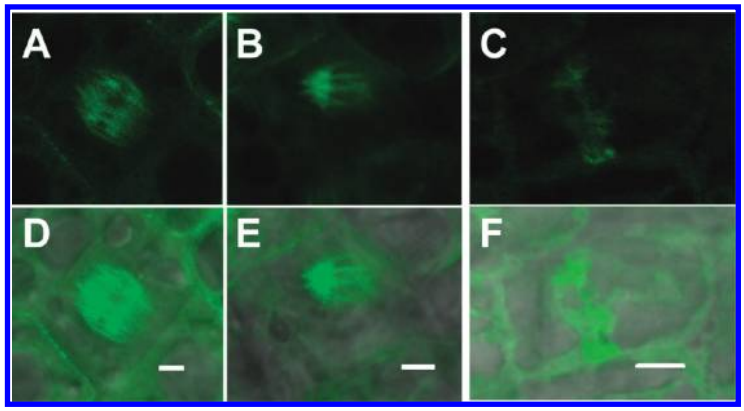

Figure 3. Fluorescence images of cortical microtubule during root cell division. The spindle of cells in the normal (A, D) and FMAD-treated (B, E) seedlings was shown, and the newly formed daughter cells were asymmetrically divided in the repressed condition (C, F). Panels D−F display the overlay of optical and fluorescence images in panels A−C. The scale bar is 2 μm for A, B, D, E, and 4 μm for panels C and F.

acid), were used.[18] Auxin is an important regulator of root growth and development and is involved in cell division, elongation, and morphology determination, *etc*.[19] The distribution of auxin in the root cap was visualized by the fluorescence signal from GFP.

As shown in Figure 2, in the normal root, there is a cone-shaped auxin distribution from layer S1 to layer S3 cells in the columella root cap. The swollen root tip of the seedling treated by FMAD showed obvious auxin accumulation in layer S1 cells, indicating that the auxin transportation was hindered in the roots.

FMAD Disrupted the Cell Division in the Meristematic Zone. Cell division is a very important event in root growth. We thus checked the meristematic zone, which is just behind the root cap. This zone is the region of cell division that supports root elongation. The mitotic cells in this region were imaged using the seedlings expressing GFP tagged β-tublin, a component of spindle formed during cell division.

As shown in Figure 3, the cell division was abnormal in the roots grown in the FMAD-containing medium. The spindle was oblique and asymmetric, in contrast to the control, which was symmetrically arrayed at right angles to the cell long axis. The misoriented and aberrant spindle arrays would be deleterious for the completion of cytokinesis during the cell division. As a result, the newly formed daughter cells were unequally divided. The aberrant cell division was consistent with the observation of disrupted auxin distribution.

FMAD Disrupted the Microtubule Arrangement in the Elongation Zone. With the seedlings expressing β-tubulin-GFP, we further checked the structure of the microtubule cytoskeleton in the epidermal cells in the root elongation zone, the region next to the meristematic zone. Microtubule is not only intimately involved in many aspects of cell differentiation and plant development, but also plays an active role in modulating the response of plants to environmental change.[20]

As shown in Figure 4, the disorganization of the cortical microtubule in the root cells was evident in the FMAD-repressed seedlings. The microtubules displayed either oblique or discrete orientation. In contrast, under the same conditions except no FMAD treatment, the cortical microtubules in the root cells aligned perpendicular to the growth axis, with only a few oblique.

FMAD Decreased the Activity of Cell in the Root Tip. After observing the characteristic changes of root features at the cellular level in different root zones, we examined the two main physiological features of the whole root tip, the cellular reactive oxygen species (ROS) and the mitochondrial activity. In plants, reactive oxygen species are generated in the electron transport processes, such as photosynthesis and respiration.[21] They play a crucial role in many cellular responses and signaling pathways.[22] Mitochondria constitute a major source of reactive oxygen species and have been proposed to integrate the cellular responses to stress.[23]

To know whether FMAD disrupts the ROS in the seedling root, 5-day old seedlings grown with 0.01 mg/mL FMAD or without FMAD were stained with 2′,7′-dichlorofluorescein diacetate, which would become fluorescent dichlorofluorescein (DCF) after reacting with ROS. The root tips were imaged and the mean fluorescence intensities were calculated. A decrease in fluorescence intensity was observed in the root cells treated with FMAD, suggesting that FMAD caused the reduction of intracellular ROS (Figure 5). As these seedlings

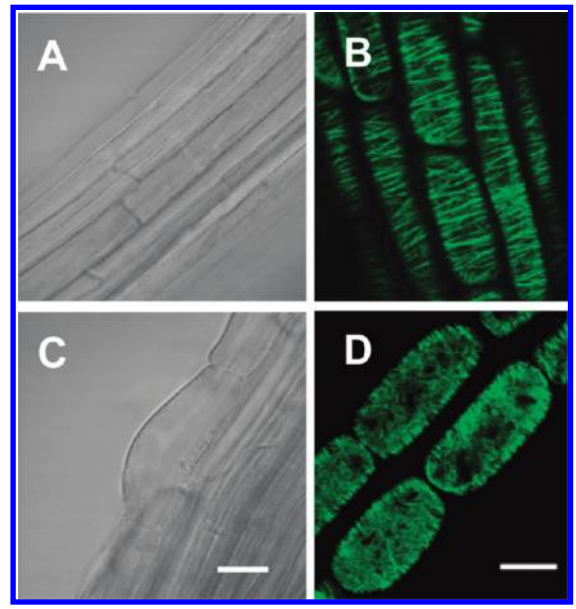

Figure 4. Images of the elongation zone in the root of the seedlings grown in the medium without (A, B) and with (C, D) 0.01 mg/mL FMAD. Both optical (A, C) and fluorescence (B, D) images are shown. The scale bar is 20 μm for panels A and C, and 10 μm for panels B and D.

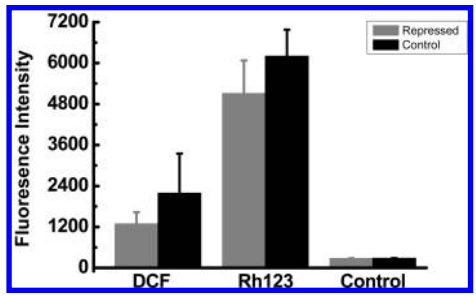

Figure 5. Mean fluorescence intensity of the seedlings root tips grown in medium with (gray) and without (black) 0.01 mg/mL FMAD. The roots were stained with 2′,7′-dichlorofluorescein diacetate and Rhodamine 123 (Rh123), respectively. Seedling roots without dye-staining were used as controls.

did not manifest any signs of damage and were viable when placed back onto agar plates after fluorescence imaging (data not shown), the ROS decrease was the consequence of FMAD treatment rather than cytotoxic response to sample manipulations, such as taking out the seedlings and washing their roots. The effect of FMAD is different from that of multiwalled carbon nanotubes which, in contrast, could increase the ROS content in suspension rice cells.[24] Furthermore, we analyzed the activity of the mitochondria by Rhodamine123.[25] Rhodamine 123 is a cell-permeant, cationic, fluorescent dye that is readily sequestered by active mitochondria without inducing cytotoxic effects. As shown in Figure 5, a decrease in fluorescence intensity in the roots of repressed seedlings was obvious, indicating the decreased activity of mitochondria.

FMAD Adhered to the Normal Seedling Roots but Internalized into the Repressed Roots. According to previous studies, nanoparticles exert their effects on plant growth either by their internalization to the plant cells or by just adherence to the cell walls.[5,7,26] We therefore investigated whether FMAD could enter the root cells. FMAD labeled with fluorescein cadaverine dye was used to visualize the location of fullerene in the root cells under a fluorescence microscope.

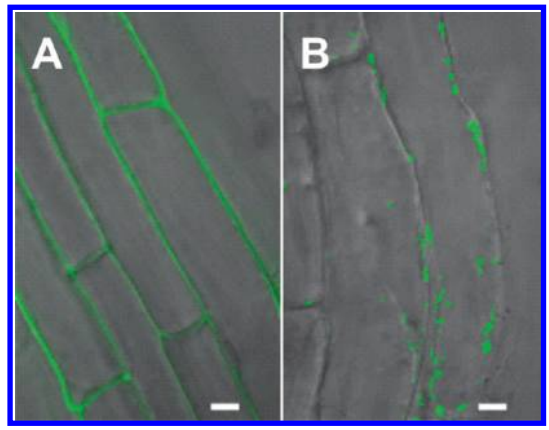

Figure 6. Overlay of the fluorescence and optical images of root cells in the 5-day old seedlings incubated with fluorescent FMAD. The seedlings grown in normal medium (A) or the medium containing 0.01 mg/mL FMAD (B) were used. The scale bar is 5 μm.

As demonstrated in Figure 6, when the fluorescent FMAD was incubated with 5-day old seedlings that had been grown in the normal medium, no fluorescence signal was found inside the root cells, whereas the fullerenes were found to be only adherent to the cell walls. However, if the 5-day old seedlings grown in the medium containing 0.01 mg/mL FMAD were used, several fluorescent spots inside the root cells of seedlings were observed (Figure 6B). We also stained these cells with Propidium Iodide (PI), a dye used to identify the integrity of cell membrane (PI enters into nucleus and fluoresces if passing through the cell membrane). The result showed that PI was excluded outside the cells, indicating that the root cortical cell membrane was not damaged by FMAD supplemented in culture medium (Figure S4, Supporting Information). Therefore, the internalization of FMAD was not due to the deficient cell wall or membrane of the root cells.

There have been reports on the internalization of nanoparticles (MWNT and ZnO) in seeds and roots, indicating nanomaterials can enter into the root of seedlings by increasing the permeability of plant cell walls and possibly creating "holes" or "pores" on the walls.[6,7] In this study, we have demonstrated the water-soluble fullerene FMADs have a negative effect on plant development, especially the root growth. It is expected that both the adherent and internalized FMAD contributed to the observed inhibitory effect. FMAD were adherent to the seedling root surface in the beginning, then it could enter into the root cells of the repressed seedlings. It is likely that the adherence of FMAD changed the structure or permeability of cell walls to facilitate FMAD internalization.[6,7] This implies that the cytotoxicity derived from the increased permeability of root cells to FMAD.

It is important to find that the adherence and internalization of FMAD resulted in the aberrant microtubule arrangement and cell division of root cells. Normal plant growth requires highly dynamic polymerization and depolymerization of microtubules.[27] When the dynamics of depolymerization and polymerization were interrupted in the abnormal microtubule arrangement, cell development would be repressed. Moreover, the plant cytoskeleton is directly involved in the intracellular transport of a wide variety of macromolecules, vesicles, and organelles, which are essential to plant growth and development.[27] It is also noteworthy that the internalization of FM4-64 dye through endocytosis was inhibited after FMAD treatment (Figure S5, Supporting Information), which is mostly due to the abnormal microtubule arrangement.[28] Therefore, the disrupted auxin gradient in the root cap would be associated with the distorted microtubules and the repression of endocytosis.[29] The abnormal auxin accumulation, together with disrupted microtubule arrangement led to the aberrant spindle during cell division. Furthermore, the disrupted cell division also hindered the root growth. On the other hand, the disorganized cortical microtubule in the FMAD re-

pressed plant could not efficiently direct the orientation of mitochondria in the root cells,[30] thus making the mitochondria less active. Of course, the detailed mechanism of how FMAD affects the microtubule alignment as well as root growth needs further investigation.

CONCLUSION

In conclusion, we have found, for the first time, that water-soluble fullerene has exerted an inhibitory effect on plant growth, particularly in seedling roots with shortened length and loss of gravitropism. By *in vivo* fluorescence imaging of the root cells in the transgenic plants, new phytotoxic effects have been revealed at the cellular level, such as auxin disruption, abnormal cell division, and microtubule disorganization. It is proposed that these phytotoxic effects would cause the lower ROS content and reduced mitochondrial activity in roots for plant development, as well as the retarded root growth in morphology. This work provides new insights to advance our understanding of the phytotoxicity mechanism of nanomaterials.

MATERIALS AND METHODS

Preparation and Characterization of the Water-Soluble Fullerene. Fullerene malonic acid derivative (FMAD), $C_{70}(C(COOH)_2)_{4-8}$, was prepared according to the previously reported method with minor modifications.[16] Briefly, C_{70} fullerene (synthesized in our lab and purified by HPLC with the purity above 98%) was converted into fullerene ester following treatment with diethyl bromomalonate (Sigma-Aldrich) and 1, 8-diazobicyclo[5,40]undec-7-ene (Alfa-Aesar) in dry toluene under nitrogen. MALDI-TOF mass spectrum (AutoFlex III, Bruker, Germany) showed the product had 4 to 8 ester groups on the fullerene cage. The fullerene ester was then converted into water-soluble fullerene acid by hydrolysis. The attachment of the carboxyl group was confirmed by Fourier transform infrared spectroscopy (FTIR, Tensor 27, Bruker, Germany). The size of the synthesized $C_{70}(C(COOH)_2)_{4-8}$ was characterized by dynamic light scattering (Nano-ZS ZEN3600, Malvern Instruments, Germany) and atomic force microscopy (NanoScope IIIa, Veeco, US) operating in the tapping mode on mica substrates.

Plant Material and Fullerene Treatment. *Arabidopsis thaliana* ecotype Columbia (Columbia [Col-0] ecotype) seeds were surface-sterilized by 8% NaClO solution (in 95% alcohol), washed four times with 95% alcohol to remove extra NaClO, and dried before use.[31] The seeds were sown on half-strength MS agar plates (Sigma-Aldrich, St. Louis, MO). The agar was formed in the medium supplemented with or without FMADs. Seeds were grown under the following conditions: 16 h/8 h light/dark; light intensity 280 μmol m^{-2} s^{-1}; temperature 25 °C/20 °C; and 70% humidity. The 5-day old seedlings were used in this study unless specified as the radicles usually started to appear in the second day and the repressed symptoms were shown clearly on the fifth day. Seedling length was measured from the digital images using the Image J software. The seeds of GFP tagged β-tubulin were kindly provided by Prof. Ming Yuan at Chinese Agricultural University (Beijing, China). The *proDR5::GFP* transformed *Arabidopsis* was made according to the method described by Friml.[32]

Assay for Root Gravitropism. Seeds were sterilized and vernalized in the dark at 4 °C for 24 h and then germinated on the plates in the medium under culture condition with or without 0.01 mg/mL FMAD. The plates were maintained vertically and the seedlings were allowed to grow vertically for the first 5 days. Then, the plates were turned through 90° and the seedlings grew for another 3 days before examining the reorientation of root growth.[33]

Fluorescence Imaging and Analysis. Seedlings were taken out of the agar plate, washed, and placed onto a glass coverslip for microscopic imaging with a drop of culture medium to keep the seedlings alive. For fluorescence and light microscopic images, cells in different sections of the root tips were imaged by a FV 1000-IX81 Confocal Laser Scanning Microscope (Olympus, Japan). A 10× objective (NA 0.3, UPlanF1, Olympus, Japan) was used for low magnification images and a 100× objective (NA 1.40, oil immersion, UPlanSpo, Olympus, Japan) was used for high magnification images.

For fluorescence intensity calculations, confocal images were first obtained with an inverted fluorescence microscope (Olympus IX71, Japan), which was equipped with a CSU10 spinning disk confocal laser-scanner unit (Yokogawa Electronic, Tokyo). The cells were excited at 488 nm from an argon ion laser (Melles Griot, CA) and the fluorescence signals were directed to an electron multiplying charge-coupled device (EMCCD) (Andor, BT). Then the image analysis and fluorescence intensity calculation was processed by IQ live cell imaging software (Andor, BT) and Image-Pro Plus 6.0 software.

Detection of ROS and Mitochondria Activity of Root Cells. The seedling roots were stained by 2′,7′-dichlorofluorescin diacetate (DCFH-DA, Sigma-Aldrich) to detect ROS production and by Rhodamine123 (Sigma-Aldrich) to detect mitochondria activity according to the previous reports.[25,34] The normal or FMAD-repressed seedlings were incubated in the half-strength MS medium with 5 μM DCFH-DA or 8 μM Rhodamine123 in the dark for 1 h. Then the seedlings were immediately washed three times with liquid media. The root tips were imaged under the confocal microscope at room temperature, with an excitation wavelength of 488 nm. The mean fluorescence intensity was calculated by averaging the fluorescence intensities of root tips (about 20 root tips) from the images of each sample using Image-Pro Plus 6.0 software. The results were reported as mean values of triplicates.

Labeling the Fullerene with Fluorescein Cadaverine. To visualize the location of FMADs, FMADs were labeled with a fluorescent dye, fluorescein cadaverine, by a two-step method.[35] In the first step, 0.2 mL of FMAD (about 0.5 mg/mL) was mixed with 2.0 mL of pure water and sonicated for a short period of time. Then, 0.5 mL of MES buffer solution (pH 5.8, 0.5 M), 1 mL of EDC solution (freshly prepared, 7 mg/mL), and 1 mL of Sulfo-NHS solution (freshly prepared, 13 mg/mL) were added into the solution under stirring. The mixture was continually stirred for 30 min at room temperature. After that, the estered fullerenes were collected by centrifugation in the centrifugal filter (10 KD, Millipore) and washed with 50 mM MES buffer (pH 5.8) to remove excess EDC, Sulfo-NHS, and the byproducts. In the second step, the estered fullerenes were redispersed in 5 mL of 50 mM MES buffer (pH 5.8), and then 10 μL of fluorescein cadaverine solution (1 mg/mL, Invitrogen) was added. The mixture was kept stirring for 3.0 h at room temperature. The final product was collected and dialyzed (MW cut off 3500) against water for 3 days, during which water was changed five times every day to remove extra reactants.

Internalization of the Labeled Fullerene into the Root Cells. To examine whether the fluorescein cadaverine labeled fullerene was internalized into the root cells, 5-day old seedlings grown on the agar plate with the normal medium or the medium containing 0.01 mg/mL FMAD were used. After carefully being removed from the plate, the seedlings were placed in the half-strength MS medium supplemented with the fluorescent fullerene and the roots were immersed in the medium. The seedlings were kept in the medium under the culture condition without light for 3 h and the roots were washed thoroughly before fluorescence imaging.

ACKNOWLEDGMENT This work was supported by National Natural Science Foundation of China (Nos. 90713024 and 20821003), the National Basic Research Program of China (2007CB935601), and the Chinese Academy of Sciences.

Supporting Information Available: Atomic force microscopy image of FMAD aggregates and dynamic light scattering measurements of their size (Figure S1), images of seedlings grown in the normal medium for 5 days and then transferred into the medium with or without FMAD for another 7 days of growing (Figure S2), images of seedlings grown in the normal medium and the medium containing FMAD first allowed to grow for 5 days, and then the plates were turned 90° and the seedlings grew for another 3 days (Figure S3), PI staining and other control experiments (Figure S4), and FM4-64 staining of root cells at different times (Figure S5). This material is available free of charge via the Internet at http://pubs.acs.org.

REFERENCES AND NOTES

1. Oberdörster, G.; Oberdörster, E.; Oberdörster, J. Nanotoxicology: An Emerging Discipline Evolving from Studies of Ultrafine Particles. *Environ. Health Perspect.* **2005**, *113*, 823–839.
2. Fischer, H. C.; Chan, W. C. W. Nanotoxicity: the Growing Need for *in vivo* Study. *Curr. Opin. Biotechnol.* **2007**, *18*, 565–571.
3. Hillegass, J. M.; Shukla, A.; Lathrop, S. A.; MacPherson, M. B.; Fukagawa, N. K.; Mossman, B. T. Assessing Nanotoxicity in Cells *in vitro*. *Wiley Interdiscip. Rev.: Nanomed. Nanobiotechnol.* **2010**, *2*, 219–231.
4. Jia, G.; Wang, H.; Yan, L.; Wang, X.; Pei, R.; Yan, T.; Zhao, Y.; Guo, X. Cytotoxicity of Carbon nanomaterials: Single-Wall Nanotube, Multi-Wall Nanotube, and Fullerene. *Environ. Sci. Technol.* **2005**, *39*, 1378–1383.
5. Yang, L.; Watts, D. J. Particle Surface Characteristics May Play an Important Role in Phytotoxicity of Alumina Nanoparticles. *Toxicol. Lett.* **2005**, *158*, 122–132.
6. Lin, D. H.; Xing, B. S. Root Uptake and Phytotoxicity of ZnO Nanoparticles. *Environ. Sci. Technol.* **2008**, *42*, 5580–5585.
7. Khodakovskaya, M.; Dervishi, E.; Mahmood, M.; Xu, Y.; Li, Z. R.; Watanabe, F.; Biris, A. S. Carbon nanotubes Are Able To Penetrate Plant Seed Coat and Dramatically Affect Seed Germination and Plant Growth. *ACS Nano* **2009**, *3*, 3221–3227.
8. Lin, D. H.; Xing., B. S. Phytotoxicity of Nanoparticles: Inhibition of Seed Germination and Root Growth. *Environ. Pollut.* **2007**, *150*, 243–250.
9. Torney, F.; Trewyn, B. G.; Lin, V. S. Y.; Wang, K. Mesoporous Silica Nanoparticles Deliver DNA and Chemicals into Plants. *Nat. Nanotechnol.* **2007**, *2*, 295–300.
10. Liu, Q. L.; Chen, B.; Wang, Q. L.; Shi, X. L.; Xiao, Z. Y.; Lin, J. X.; Fang., X. H. Carbon nanotubes as Molecular Transporters for Walled Plant Cells. *Nano Lett.* **2009**, *9*, 1007–1010.
11. Etxeberria, E.; Gonzalez, P.; Baroja-Fernandez, E.; Pozueta-Romero, J. Fluid Phase Endocytic Uptake of Artificial Nano-Spheresand Fluorescent Quantum Dots by Sycamore Cultured Cells. *Plant Signaling Behavior* **2006**, *1*, 196–200.
12. Wang, Q. L.; Chen, B.; Liu, P.; Zheng, M. Z.; Wang, Y. Q.; Cui, S. J.; Sun, D. Y.; Fang, X. H.; Liu, C. M.; Lucas, W. J.; et al. Calmodulin Binds to Extracellular Sites on the Plasma Membrane of Plant Cells and Elicits a Rise in Intracellular Calcium Concentration. *J. Biol. Chem.* **2009**, *284*, 12000–12007.
13. Ravindran, S.; Kim, S.; Martin, R.; Lord, E. M.; Ozkan, C. S. Quantum Dots as Bio-labels for the Localization of A Small Plant Adhesion Protein. *Nanotechnology* **2005**, *16*, 1–4.
14. Yu, G.; Liang, J.; He, Z.; Sun, M. Quantum Dot-Mediated Detection of γ-Aminobutyric Acid Binding Sites on the Surface of Living Pollen Protoplasts in Tobacco. *Chem. Biol.* **2006**, *13*, 723–731.
15. Isaacson, C. W.; Kleber, M.; Field, J. A. Quantitative Analysis of Fullerene nanomaterials in Environmental Systems: A Critical Review. *Environ. Sci. Technol.* **2009**, *43*, 6463–6474.
16. Chaudhuri., P.; Paraskar, A.; Soni, S.; Mashelkar, R. A.; Sengupta, S. Fullerenol-Cytotoxic Conjugates for Cancer Chemotherapy. *ACS Nano* **2009**, *3*, 2505–2514.
17. Wierzbicka, M.; Obidzińska, J. The Effect of Lead on Seed imbibition and Germination in Different Plant Species. *Plant Sci.* **1998**, *137*, 155–171.
18. Blilou, I.; Xu, J.; Wildwater, M.; Willemsen, V.; Paponov, I.; Friml, J.; Heidstra, R.; Aida, M.; Palme, K.; Scheres, B. The PIN Auxin Efflux Facilitator Network Controls Growth and Patterning in *Arabidopsis* roots. *Nature* **2005**, *433*, 39–44.
19. Friml, J. Auxin Transport-Shaping the Plant. *Curr. Opin. Plant Biol.* **2003**, *6*, 7–12.
20. Wasteneys, G. O. Progress in Understanding the Role of Microtubules in Plant Cells. *Curr. Opin. Plant Biol.* **2004**, *7*, 651–660.
21. Rentel., M. C.; Knight., M. R. Oxidative Stress-Induced Calcium Signaling in *Arabidopsis*. *Plant Physiol.* **2004**, *135*, 1471–1479.
22. Ashtamker, C.; Kiss, V.; Sagi, M.; Davydov, O.; Fluhr., R. Diverse Subcellular Locations of Cryptogein-Induced Reactive Oxygen Species Production in Tobacco Bright Yellow-2 Cells. *Plant Physiol.* **2007**, *143*, 1817–1826.
23. Tiwari, B. S.; Belenghi, B.; Levine., A. Oxidative Stress Increased Respiration and Generation of Reactive Oxygen Species, Resulting in ATP Depletion, Opening of Mitochondrial Permeability Transition, and Programmed Cell Death. *Plant Physiol.* **2002**, *128*, 1271–1281.
24. Tan, X.; Lin, C.; Fugetsu, B. Studies on Toxicity of Multi-walled Carbon nanotubes on Suspension Rice Cells. *Carbon* **2009**, *47*, 3479–3487.
25. Lin, J.; Wang, Y.; Wang, G. Salt Stress-induced Programmed Cell Death in Tobacco Protoplasts is Mediated by Reactive Oxygen Species and Mitochondrial Permeability Transition Pore Status. *J. Plant Physiol.* **2006**, *163*, 731–739.
26. Kurepa, J.; Paunesku, T.; Vogt, S.; Arora, H.; Rabatic, B. M.; Lu, J.; Wanzer, M. B.; Woloschak, G. E.; Smalle, J. A. Uptake and Distribution of Ultrasmall Anatase TiO_2 Alizarin Red S Nanoconjugates in *Arabidopsis thaliana*. *Nano Lett.* **2010**, *10*, 2296–2302.
27. Coddard, R. H.; Wick, S. M.; Silflow, C. D.; Snustad., D. P. Microtubule Components of the Plant Cell Cytoskeleton. *Plant Physiol.* **1994**, *104*, 1−6.
28. Voigt, B.; Timmers, A. C.; Samaj, J.; Hlavacka, A.; Ueda, T.; Preuss, M.; Nielsen, E.; Mathur, J.; Emans, N.; Stenmark, H.; et al. Actin-Based Motility of Endosomes is Linked to the Polar Tip Growth of Root Hairs. *Eur. J. Cell Biol.* **2005**, *84*, 609–621.
29. Robert, H. S.; Friml., J. Auxin and Other Signals on the Move in Plants. *Nat. Chem. Biol.* **2009**, *5*, 325–332.
30. Yi, M.; Weaver, D.; Hajnoczky, G. Control of Mitochondrial Motility and Distribution by the Calcium Signal: A Homeostatic Circuit. *J. Cell Biol.* **2004**, *167*, 661–672.
31. Xiang, C.; Oliver, D. J. Glutathione Metabolic Genes Coordinately Respond to Heavy Metals and Jasmonic Acid in *Arabidopsis*. *Plant Cell* **1998**, *10*, 1539–1550.
32. Benkova, E.; Michniewicz, M.; Sauer, M.; Teichmann, T.; Seifertova, D.; Jurgens, G.; Friml, J. Local, Efflux-Dependent Auxin Gradients as a Common Module for Plant Organ Formation. *Cell* **2003**, *115*, 591–602.
33. Marchant, A.; Kargul, J.; May, S. T.; Muller, P.; Delbarre, A.; Perrot-Rechenmann, C.; Bennett, M. J. AUX1 Regulates Root Gravitropism in *Arabidopsis* by Facilitating Auxin Uptake Within Root Apical Tissues. *EMBO J.* **1999**, *18*, 2066–2073.
34. He, Y. Y.; Häder, D. P. UV-B-induced Formation of Reactive Oxygen Species and Oxidative Damage of the Cyanobacterium *Anabaena* sp.: Protective Effects of Ascorbic Acid and N-acetyl-L-cysteine. *J. Photochem. Photobiol. B* **2002**, *66*, 115–124.
35. Jiang, K.; Schadler, L. S.; Siegel, R. W.; Zhang, X.; Zhang, H.; Terrones, M. Protein Immobilization on Carbon nanotubes via A Two-step Process of Diimide-activated Amidation. *J. Mater. Chem.* **2004**, *14*, 37–39.